



Published in final edited form as:

J Neural Eng. ; 17(1): 016024. doi:10.1088/1741-2552/ab2409.

Seizure tracking of epileptic EEG using a model-driven approach

Jiang-Ling Song^{1,2}, Qiang Li^{1,2}, Min Pan¹, Bo Zhang¹, M. Brandon Westover², Rui Zhang¹

⁽¹⁾The Medical Big Data Research Center, Northwest University, Xi'an, China

⁽²⁾The Department of Neurology, Massachusetts General Hospital, Boston, MA

Abstract

Objective.—As a chronic neurological disorder, epilepsy is characterized by recurrent and unprovoked epileptic seizures which can disrupt the normal neurobiologic, cognitive, psychological conditions of patients. Therefore, it is worthwhile to give a detailed account of how the epileptic EEG evolves during a period of seizure so that an effective control can be guided for epileptic patients in clinics.

Approach.—Considering the successful application of neural mass model in exploring the insights into brain activities for epilepsy, in this paper, we aim to construct a model-driven approach to track the development of seizures using epileptic EEGs. We first propose a new time-delay Wendling model with sub-populations (TD-W-SP model) with respect to three aspects of improvements. Then we introduce a model-driven seizure tracking approach, where a model training method is designed based on extracted features from epileptic EEGs and a tracking index is defined as a function of the trained model parameters.

Main results.—Numerical results on 8 patients on CHB-MIT database demonstrate that our proposed method performs well in simulating epileptic-like EEGs as well as tracking the evolution of three stages (that is, from pre-ictal to ictal and from ictal to post-ictal) during a period of epileptic seizure.

Significance.—An useful attempt to track epileptic seizures by combining the neural mass model with the data analysis.

Keywords

Neural mass model; epilepsy; Electroencephalogram (EEG); seizure tracking

1. Introduction

As a chronic neurological disorder, epilepsy is characterized by episodic interruptions of cerebral electrical activities caused by abnormal hypersynchronous discharges of neuronal populations, which can disrupt the normal neurobiologic, cognitive, psychological conditions of patients [1]. Electroencephalography (EEG) is a technique for recording and

rzhang@nwu.edu.cn.

Conflict of interest statement

None Declared.

interpreting the electrical activity of the brain, which measures voltage fluctuations resulting from ionic current within the brain neurons[2]. Due to its high temporal resolution, EEG is one of the effective and widely used tools to investigate epilepsy.

With the development of emerging information technologies such as machine learning, data mining etc., there have been explored various disease-oriented and data-based methods aiming to realize the auxiliary diagnosis, early warning and pre-control. The automatic epileptic seizure detection, which is one of the most representative applications, has been designed to solve the time-consuming and subjective problems caused by visual inspection of long-term EEGs in clinics [2, 3, 4, 5, 6, 7, 8, 9]. In general, the seizure detection is modeled as a binary classification problem where two states (seizure and non-seizure) are considered. However, the evolution of seizure is actually a continuous process which mainly includes three stages (pre-ictal, ictal, and post-ictal) †. Therefore, such data-based seizure detection methods cannot give a detailed account of how the epileptic EEG evolves during a period of seizure, which is valuable in guiding the effective control for epilepsy patients in clinics.

Neural mass model (NMM), which is one of the most popular neural computational models, informs us about the dynamics resulting from the interactions between multiple brain regions such as the cortex, thalamus and brain stem. Different from single neuronal model, NMM considers the average activity of interconnected populations without explicit representation of mechanisms lying at cellular level. Neurons in each population share the similar electrophysiological properties, which mainly include pyramidal neurons or interneurons. In applications, NMMs are often used to discover the underlying mechanisms of physiological behaviors, which can further reveal intrinsic characteristics of complex data, or test hypotheses corresponding to some new discoveries. Originated from the Beurle's work in early 1950s [11], a large amount of NMMs have been developed to finish various explorations such as explaining the generation of α rhythm in the thalamus [12], studying the neural oscillations' synchronization [13], interpreting various physiological and pathological phenomenon [14, 15, 16, 17, 18, 19] and so on.

Regarding to epilepsy, Wendling et al. proposed a novel NMM where two types of interneurons populations (i.e., $GABA_{A,fast}$ and $GABA_{A,slow}$) were considered due to the respective role of dendritic-projecting and somatic-projecting interneurons [20]. As a result, the hippocampal dynamics were simulated during epileptic seizures by the model [14]. With the recognition that Wendling model could explore the insights into brain activities for epilepsy, it is definitely a good attempt to construct a model-driven approach, by which how EEG evolves during a period of epileptic seizure is studied. In this paper, we will first propose a time-delay Wendling model with sub-populations (TD-W-SP model) in three aspects of improvements: (1) a new response function is formulated in pyramidal population; (2) two time delays are added in excitatory interneuron population and slow inhibitory interneuron population; and (3) each population are divided into a number of sub-populations. Then a model-driven seizure tracking approach will be introduced where the

†Conceptually, the pre-ictal stage is described by the period of specific brain activity leading to an actual seizure, and the post-ictal stage may be reflected by generally suppression of background activity or increased slow activity[10].

TD-W-SP model is trained according to two features extracted from epileptic EEGs, as well as the model parameter variation trend is characterized to explore the evolution of three stages during a period of epileptic seizure.

The architecture of this paper is as follows. In section II, we present a new time-delay Wendling model with sub-populations and a model-driven seizure tracking approach using epileptic EEGs. Then we present the experimental results on CHB-MIT database in section III. Some concluding remarks are given in the last section.

2. Method

This section will first introduce a new time-delay Wendling model with sub-populations (TD-W-SP model) followed by an overview of Wendling model. Then a model-driven seizure tracking approach will be proposed systematically.

2.1. A new time-delay Wendling model with sub-populations

A1) Overview of Wendling model—In 2000, a neurophysiological finding revealed that two types of $GABA_A$ synaptic responses, that is, a fast one near the soma and a slow one in the dendrites, may play crucial roles in the formation of gamma rhythms in pyramidal cells [21]. Such two types of responses come from two types of GABAergic inhibition interneurons, which are dendritic inhibition interneurons (denoted by $GABA_{A,slow}$) and somatic inhibition interneurons (denoted by $GABA_{A,fast}$) respectively. Originated from this finding, Wendling et al. [20] proposed a neural mass model to study the generation of high-frequency EEG activities in 2002, where the inhibition interneuron population was replaced by considering two populations (that is, $GABA_{A,fast}$ and $GABA_{A,slow}$) in the existing model proposed by Jansen & Rit [22]. For convenience, we name this model as “Wendling model” in what follows. Fig. 1 illustrates the topological structure of Wendling model. There include four populations in the model: the pyramidal population (PY), the excitatory interneuron population (E), the slow dendritic inhibitory interneuron population (I1) and the fast somatic inhibitory interneuron population (I2). Among four populations, PY receives postsynaptic firing rate from E, I1 and I2, as well as send postsynaptic potential (PSP) to E, I1 and I2. Meanwhile, population I2 also receive postsynaptic firing rate from I1 due to the physiological connection between them.

In each population, the dynamics evolution is formulated by two operators. The first one is a convolution operator where the firing rate $m(t)$ is mapped into the PSP $v(t)$, that is,

$$v(t) = h(t) \otimes m(t). \quad (1)$$

In Eq. (1), the response function $h(t)$ corresponds to three cases: excitatory h_e , slow inhibitory h_i , fast inhibitory h_f which are denoted by

$$h_e(t) = Aate^{-at}, t \geq 0, \quad (2)$$

$$h_i(t) = Bbte^{-bt}, t \geq 0, \quad (3)$$

$$h_f(t) = Ggte^{-gt}, t \geq 0. \quad (4)$$

Here, A , B and G denote the synaptic gains, a , b and g are the lumped representation of time constants.

Conversely, the second operator transforms the PSP $v(t)$ into the firing rate $m(t)$, which is always selected to be a sigmoid function. It is generally described by

$$S(v(t)) = \frac{2e_0}{1 + e^{r(v_0 - v(t))}} \quad (5)$$

where e_0 is the maximum firing rate, v_0 is the firing threshold and r is the steepness of the sigmoidal transformation.

Since it is difficult to calculate the operator “ \otimes ” in a direct way, the Laplace transformation is applied so that Eq. (1) could be re-expressed by a pair of first order ordinary differential equations equivalently, that is,

$$\begin{aligned} \dot{v}(t) &= v_1(t), \\ \dot{v}_1(t) &= \Gamma\gamma m(t) - 2\gamma v_1(t) - \gamma^2 v(t). \end{aligned} \quad (6)$$

Here, $\Gamma \in \{A, B, G\}$ and $\gamma \in \{a, b, g\}$. Fig. 2(a) illustrates the computational block in each population.

A2) the time-delay Wendling model with sub-populations—Wendling model broke a new ground in the field of NMM due to the successful design by considering two types of GABAergic inhibition interneurons, that is, $GABA_{A,fast}$ interneurons (I2) and $GABA_{A,slow}$ interneurons (I1). However, there lacks of concerning the response alteration of population PY when it interacts with I1 and I2 respectively. Meanwhile, with the recognition that time delay in neuronal signal transmission is a key factor to cause seizures [23], there lacks of concerning the response alteration of populations E and I1, which are influenced by the entry of time delays in connections. For the sake of keeping modeling more flexibility in producing epileptiform activities, the computational blocks in populations should be re-formulated mathematically under new considerations. In addition, the neurons in the same type of population may have different responses for the same stimulus [24], which means various sub-populations with their own kinetics should be included in one population. And it will be more effective in capturing the diversity of neuronal networks. Motivated by such recognition, a new time-delay Wendling model with sub-populations (TD-W-SP model) will be proposed in this paper.

We first consider the case of pyramidal population, which can be regarded as a central hub in the construction of NMMs. In the original Wendling model, it accounts for the same response function for population PY when it interacts with populations I1 and I2 respectively, which means PY sends PSP into I1 and I2 in the same way. However, two

situations should be addressed on PY in light of considering the different characteristics of $GABA_{A,slow}$ and $GABA_{A,fast}$. Specifically, we have

$$h_e^{PY}(t) = \begin{cases} Aate^{-at}, & \text{if PY} \rightarrow \text{E/I1}; \\ A'a'te^{-a't}, & \text{if PY} \rightarrow \text{I2}. \end{cases} \quad (7)$$

Here, $h_e^{PY}(t)$ represents the response function of PY in TD-W-SP model with different parameters (A, a) and (A', a') under two situations. Fig. 2(b) illustrates the computational block of PY with new formulation.

Next, we consider the case of interneuron population. In [23], Geng et al. added an additional time-delay in the inhibitory feedback loop, and to simulate several different types of EEG activity including alpha wave and ictal EEG. This work succeeded in showing that the time delay in neuronal signal transmission is a key factor to cause seizures. Originated from this work, in order to further account for the impaired balance between excitatory and inhibitory populations, the time delay τ_a and τ_b are added both in the excitatory and inhibitory feedback loop. Based on these points, we formulate the computational blocks with time delay in E and I1 as

$$h_e^E(t) = \delta(t - \tau_a)Aate^{-at}, \quad (8)$$

$$h_i(t) = \delta(t - \tau_b)Bbte^{-bt}, \quad (9)$$

$$t \geq 0, \tau \geq 0 \quad (10)$$

where τ_a and τ_b denote the time delays existing in the connections between PY and E, as well as PY and I1 respectively, $h_e^E(t)$ represents the excitatory response of E in TD-W-SP model. Fig. 2(c) illustrates the time-delay computational block.

Finally, according to [4], David et.al. revealed that the neurons in the same type of population may have different responses for the same stimulus, and verified that Jansen & Rit model could capture more complex dynamics of a neural system if each population is extended by N parallel subpopulations with different kinetics. Motivated by such recognition, in this work, we divided each population into N sub-populations deploying in parallel with different kinetics, whose structure is shown in Fig. 2(d). Assume that v_1, v_2, \dots, v_N are the outputs and w_1, w_2, \dots, w_N the weights of sub-populations, then the final output of the population is formulated to be the weighted sum of them, that is,

$$v = w_1v_1 + w_2v_2 + \dots + w_Nv_N. \quad (11)$$

By combining above modifications (say, Eqs. (7)–(11)) with Wendling model, the mathematical formulation of TD-W-SP model in the case of $N=2$ can be represented by Eq. (12) (see page 5). Fig. 3 illustrates the neuronal population organization of TD-W-SP model.

The final model output is the weighted sum of membrane potential of two excitatory sub-populations and four inhibitory sub-populations $wv_2 + (1 - w)v_8 - wv_3 - (1 - w)v_9 - wv_6 - (1 - w)v_{12}$.

2.2. A model-driven seizure tracking approach using epileptic EEGs

In this subsection, we will introduce a model-driven seizure tracking approach where the TD-W-SP model is first trained according to two features extracted from epileptic

$$\begin{aligned}
\ddot{v}_1(t) &= AaS(wv_2(t - \tau_a) + (1 - w)v_8(t - \tau_a) - wv_3(t - \tau_b) - (1 - w)v_9(t - \tau_b) \\
&\quad - wv_6(t) - (1 - w)v_{12}(t)) - 2a\dot{v}_1(t) - a^2v_1(t); \\
\ddot{v}_2(t) &= AaC_2S(C_1(wv_1(t) + (1 - w)v_7(t))) - 2a\dot{v}_2(t) - a^2v_2(t) + Aap(t); \\
\ddot{v}_3(t) &= BbC_4S(C_3(wv_1(t) + (1 - w)v_7(t))) - 2b\dot{v}_3(t) - b^2v_3(t); \\
\ddot{v}_4(t) &= A'a'S(wv_2(t - \tau_a) + (1 - w)v_8(t - \tau_a) - wv_3(t - \tau_b) - (1 - w)v_9(t - \tau_b) \\
&\quad - wv_6(t) - (1 - w)v_{12}(t)) - 2a'\dot{v}_4(t) - a'^2v_4(t); \\
\ddot{v}_5(t) &= BbC_6S(C_3(wv_1(t) + (1 - w)v_7(t))) - 2b\dot{v}_5(t) - b^2v_5(t); \\
\ddot{v}_6(t) &= GgC_7S(wv_4(t) + (1 - w)v_{10}(t) - wv_5(t) - (1 - w)v_{11}(t)) - 2g\dot{v}_6(t) - g^2v_6 \\
&\quad (t); \\
\ddot{v}_7(t) &= A_1a_1S(wv_2(t - \tau_a) + (1 - w)v_8(t - \tau_a) - wv_3(t - \tau_b) - (1 - w)v_9(t - \tau_b) \\
&\quad - wv_6(t) - (1 - w)v_{12}(t)) - 2a_1\dot{v}_7(t) - a_1^2v_7(t); \\
\ddot{v}_8(t) &= A_1a_1C_2S(C_1(wv_1(t) + (1 - w)v_7(t))) - 2a_1\dot{v}_8(t) - a_1^2v_8(t) + A_1a_1p(t); \\
\ddot{v}_9(t) &= B_1b_1C_4S(C_3(wv_1(t) + (1 - w)v_7(t))) - 2b_1\dot{v}_9(t) - b_1^2v_9(t); \\
\ddot{v}_{10}(t) &= A'_1a'_1S(wv_2(t - \tau_a) + (1 - w)v_8(t - \tau_a) - wv_3(t - \tau_b) - (1 - w)v_9(t - \tau_b) \\
&\quad - wv_6(t) - (1 - w)v_{12}(t)) - 2a'_1\dot{v}_{10}(t) - a_1'^2v_{10}(t); \\
\ddot{v}_{11}(t) &= B_1b_1C_6S(C_3(wv_1(t) + (1 - w)v_7(t))) - 2b_1\dot{v}_{11}(t) - b_1^2v_{11}(t); \\
\ddot{v}_{12}(t) &= G_1g_1C_7S(wv_4(t) + (1 - w)v_{10}(t) - wv_5(t) - (1 - w)v_{11}(t)) - 2g_1\dot{v}_{12}(t) \\
&\quad - g_1^2v_{12}(t);
\end{aligned} \tag{12}$$

EEGs, and then an index is defined as a function of trained parameters to track the evolution of seizures in epileptic EEGs.

With the extracted features from EEGs, epileptic seizures can be detected automatically by solving a binary classification problem. However, such method could only differentiate ictal EEGs from non-ictal EEGs, but is hard to give more detailed information on further capturing the transition among pre-ictal, ictal and post-ictal EEGs. Fortunately, neural computational models (NCMs) provide a potential way to explore the insights into brain activities, and a number of NCMs have been developed to elucidate the generation of physio-pathological activities, whose parameters can be explicitly related to neurological mechanisms or physiological processes (that are potentially unidentified) [14, 15, 16, 18, 20, 25, 26, 27, 28]. It implies that tracking the variation of model parameters may be a better way to further understand the evolution of epilepsy.

Although such physiology-based computational models are promising in explaining the underlying mechanisms for epilepsy, they often neglect the information contained in clinic

epileptic EEGs. Hence there exists a big gap between the model and its application in clinics. Fortunately, we can collect EEGs from epilepsy patients. Therefore, in this work, a model training method was designed by combining the strong points of model with EEG analysis, where the determination of model parameters are guided by real epileptic EEGs. Obviously, such obtained model parameters and its variation could help to understand the change of EEG signals during epilepsy, as well as the mechanisms of seizure transitions.

First of all, we describe two features extracted from epileptic EEGs. It is well known that the power spectra increases when seizures are occurring, and the dominant range of frequency for epileptic seizures is $[0, 30]$ Hz according to the acknowledgement by neurologists [2]. Therefore, given an EEG signal S , we calculate the power spectra of S by multi-taper method [29], and take those located in $[0, 30]$ Hz to be the first extracted feature, denoted by \mathbf{F}_1 (the detail calculations could be seen in Supplementary). Fig. 4 (a) illustrates the power spectral located in $[0, 30]$ Hz of pre-ictal, ictal and post-ictal EEGs. Seen from Fig. 4(a), it can be concluded that the first extracted feature \mathbf{F}_1 is able to differentiate such three stages during a seizure. In addition, with the recognition that EEGs in inter-ictal periods are more complex than those in ictal periods, we apply the fractal dimension to be another extracted feature [30], denoted by \mathbf{F}_2 (the detail calculations could be seen in Supplementary). Fig. 4(b) illustrates the fractal dimension on pre-ictal, ictal and post-ictal EEGs. We can observe that the fractal dimension on ictal EEGs is generally lower than that on pre-ictal and post-ictal EEGs, which is consistent with the above recognition. Write the fusion feature as $\mathbf{F} = (\mathbf{F}_1^T, \mathbf{F}_2^T)^T$.

Next, we present a model training method based on the extracted features and genetic algorithm (MTM-F-GA). Let $V(\Theta)$ be the output of TD-W-SP model provided that the parameter vector Θ is given. Denote by $\mathbf{F}(S)$, $\mathbf{F}(V)$ the corresponding extracted features, we define an error function between the real EEG signal S and the model output $V(\Theta)$ as

$$E(\Theta) = 1 - C(\mathbf{F}(S), \mathbf{F}(V)) \quad (13)$$

where $C(\cdot, \cdot)$ represents the cosine similarity. Applying genetic algorithm (GA) [31] to find the optimal solution Θ^* of the minimization problem

$$\min_{\Theta} E(\Theta), \quad (14)$$

we then obtain the simulated EEG signal $V(\Theta^*)$ related to S .

Finally, we apply $V(\Theta^*)$ to explore the evolution of seizures in EEG signal S . As reported in most literatures, different parameters in the TD-W-SP model have various contributions to seizure onset as well as its development. Comparing with other parameters, it has been reported in [32] that the excitation gains (i.e., A or A') and inhibition gains (i.e., B or G) play central roles in the transition between the normal EEG activity and a seizure. Moreover, the influence of a delay on the model's dynamical behavior has been analyzed in [23]. The results revealed that transmission delays among neurons (i.e., τ) may make seizures more easily be produced when they reach a certain degree. In order to avoid un-identifiability of the system due to the redundancy of parameters, in this paper, we only consider A , B , τ_a , τ_b

being variable, while other parameters setting nominal values[‡]. According to [33], one possible physiological alteration in epilepsy was summarized as follows. Before seizures are going to occur (pre-ictal) the excitatory activities become strong and the inhibitory activities become weak simultaneously; as seizures continue (ictal), such trend appear more and more pronounced; however, when seizures are coming to an end (post-ictal), the excitatory and the inhibitory activities get recovered to their normal state gradually. With such recognition, the variation trend of A , B , τ_a , τ_b can be very helpful in guiding us to explore the evolution of seizures. Let $I = f(A, B, \tau_a, \tau_b)$ be a combination of four parameters. We segment the EEG signal S into a number of EEG segments, denoted by S_1, S_2, \dots, S_N . For each EEG segment S_i , we can find the corresponding optimal solution Θ^* . Calculate $I_i = f(A_i^*, B_i^*, \tau_{a_i}^*, \tau_{b_i}^*)$, then we obtain an index sequence $\{I_1, I_2, \dots, I_N\}$. The trend of such sequence just corresponds to the evolution of seizures, that is, from pre-ictal to ictal and then from ictal to post-ictal.

In this work, we define

$$I(A, B, \tau_a, \tau_b) = \frac{\log(A/\tau_a)}{\log(B/\tau_b)}. \quad (15)$$

Here, parameters A and B are set to belong to $[3, 30]$ mV and $[0, 50]$ mV respectively according to the work of [20], as well as parameters τ_A and τ_B are set to belong to $[0.1, 5]$ ms according to the work of [23]. Obviously, the defined index is able to measure the relative proportion between excitation and inhibition of the system. Then for segments $\{S_1, S_2, \dots, S_N\}$, we denote by $\left\{ \left(A_n^*, B_n^*, \tau_{a_n}^*, \tau_{b_n}^* \right) \right\}_{n=1}^N$ the sequence of optimal parameters and by $\left\{ I_n = I \left(A_n^*, B_n^*, \tau_{a_n}^*, \tau_{b_n}^* \right) \right\}_{n=1}^N$ the sequence of indexes of them. In order to measure the trend of $\{I_n\}_{n=1}^N$, we further define two thresholds λ_1 and λ_2 . Select a sequence of normal EEG signals, $\{\mathcal{X}_1, \mathcal{X}_2, \dots, \mathcal{X}_{K_{nor}}\}$, we calculate the indexes of them by (15), denoted by $\{I_1^{nor}, I_2^{nor}, \dots, I_{K_{nor}}^{nor}\}$, and define

$$\lambda_1 = \text{mean} \left\{ I_1^{nor}, I_2^{nor}, \dots, I_{K_{nor}}^{nor} \right\}, \quad (16)$$

$$\lambda_2 = \text{mean} \left\{ I_1^{nor}, I_2^{nor}, \dots, I_{K_{nor}}^{nor} \right\} + \text{var} \left\{ I_1^{nor}, I_2^{nor}, \dots, I_{K_{nor}}^{nor} \right\}. \quad (17)$$

According to these two thresholds, the two turning points, from pre-ictal to ictal (TP-PI) and from ictal to post-ictal (TP-IP), are defined to track the evolution of seizures. TP-PI is defined by TP-IP is defined by

[‡]Here, we assume that A, B, A', G play the same role in seizure tracking. The proposed method also can be used to analyze (A', B, τ_a, τ_b) or (A', G, τ_a, τ_b) or (A, G, τ_a, τ_b)

$$\mathbf{TP}_{PI} = \min_{k_1+1 \leq k \leq K} \left\{ k: I_{k-k_1} \geq \lambda_1, \dots, I_k \geq \lambda_1 \right\}, \quad (18)$$

TP-IP is defined by

$$\mathbf{TP}_{IP} = \left\{ k: I_{k-1} - \lambda_2 \geq 0, I_k - \lambda_2 \leq 0 \right\}. \quad (19)$$

Remark 1: According to [33], one possible physiological alteration underlying epilepsy is the increased excitation and decreased inhibition of neural system. Therefore, we first define the mean value of index sequence in normal state as the baseline (that is the λ_1). When the index of a present EEG segment is larger than λ_1 , there exist an increasing trend of imbalance between excitation and inhibition. Hence, the corresponding time point is considered as the potential occurrence time of a seizure, and meanwhile, the consecutive k_1 indexes are required to be larger than λ_1 . Finally, the minimum of such k_1 time points is defined as TP_{PI} .

Reversely, the “excitation-inhibition balance” will be recovered again in a short time after the seizure is terminated. In such case, if we continue using the mean value of indexes in normal states as the baseline, then the evaluated termination time will be delayed. Therefore, we define a new baseline as λ_2 . When the index of a present EEG segment begins to be lower than λ_2 , the corresponding time point is considered as the termination time of a seizure, i.e., TP_{IP} .

The procedure of the proposed TD-W-SP model and the model-driven seizure tracking approach using epileptic EEGs can be illustrated in Fig. 5.

3. Results

3.1. EEG dataset

In this paper, we apply EEG data from CHB-MIT database into the performance verification. CHB-MIT database is collected from Boston Children Hospital, which consists of EEG recordings from 22 pediatric patients (5 males, ages 3–22; and 17 females, ages 1.5–19) with intractable seizures. Patients are monitored for up to several days following withdrawal of anti-seizure medication. Most files contain 23-channel EEG signals with sampling rate 256Hz and 16-bit resolution. In each file, EEG data are segmented into one-hour long records in most cases. All of 198 seizures are included and the corresponding onset and off set times are annotated by experts [34].

Due to the fact that the proposed TD-W-SP model is a single NCM, only one-channel EEG is available in simulations. Hence, one principle channel should be selected from multiple channels on which epileptic waveforms appear obviously. It is known that seizure is not always present in all EEG channels except the seizure onset one [35]. Therefore, we hypothesize that the onset channel is the principle channel. Then we select 8 patients whose seizure onset channel have been further stated in [35], where channel selection is based on the knowledge of the epileptic focus, and EEG recording contains multiple seizures. In our

simulation, 0.5Hz high-pass and 60Hz notch filters are applied to de-noise the data before further analysis. Then for each patient, all EEG segments including seizure are selected from its EEG recording. Since the duration of seizures are distinct, such selected EEG segments have different lengths where pre-ictal duration and post-ictal duration are set to be around 30s. Fig. 6 shows the EEG signal with two seizures from “patient 1”, and corresponding EEG signals of seizure onset channel. Since the limited space, the duration between two seizures are omitted. With the basics outlined above, the EEG dataset is finally built whose detail information are listed in Table 1, including the basic information included in 8 EEG signals (age, duration, number of channels), as well as the detailed information of constructed EEG dataset (the selected channel, number of seizures, the total duration of seizures).

3.2. Experimental results

This subsection will first verify the effectiveness of the proposed TD-W-SP model in simulating seizure-like EEGs. Then the verification results of our proposed model training method will be exhibited. Finally, the model-driven seizure tracking approach will be verified on exploring the evolution of “Preictal-ictal-Postictal” in epileptic EEGs systematically.

B1) performance verification of the TD-W-SP model—In this part, we focus on analyzing the effectiveness of the proposed TD-W-SP model in simulating seizure-like EEGs. Fig. 7 (a)–(c) illustrate the outputs of three different models, which are the original Wendling model, the Wendling model with the improved response function h_e^{PY} (abbreviated by Wendling + IRF-PY”), and the Wendling model with h_e^{PY} as well as the time delay τ_a, τ_b (abbreviated by Wendling + IRF-PY + TD”). Fig. 7 (d)–(f) illustrates three real depth-EEG signals recorded in human hippocampus (during SEEG exploration and using intracerebral multiple lead depth-electrodes) in [20]. We can observe from Figure 7 that: 1) the output of Wendling model is similar to normal background activity when all parameters are set to be their nominal values (comparing subfigures (a) and (d)); 2) the rhythmic discharges appear when the new response function h_e^{PY} is added. Here, all parameters are nominal value except that $A' = 4.25$ (comparing subfigures (b) and (d)). It resembles the slow quasi-sinusoidal activity from the morphology and rhythmicity point of view, which may be encountered during seizures [20]; 3) the seizure-like EEG signal occurs when delay factors τ_a, τ_b are additionally included when all parameters are nominal value except that $A' = 4.25, \tau_a = 0.1ms, \tau_b = 2ms$. It is analogous to the sustained discharge of spikes, which may be encountered at seizure onset or during seizures [20].

In order to further verify that model with sub-populations is good at capturing the diversity of neuronal networks, we compare the results obtained by the original Wendling model and the Wendling model with sub-populations (abbreviated by “Wendling + SP”). As shown in [20], the original Wendling model could produce two types of waveforms with different combination of parameters $(B, G) \in [0, 50] \times [0, 30]$ and $A = 3$, which are simulated normal background activity and slow rhythmic activity (i.e. “type 1” and “type 2” in Fig. 8 (a)). However, we can observe that the “Wendling + SP” could produce four types of waveforms

under the same assumptions of parameters (i.e. all sub-figures “type 1-type 4” in Fig. 8 (a)), where type 3 corresponds to the simulated sustained discharge of spikes and type 4 corresponds to slow quasi-sinusoidal activity. These results validate that the Wendling model with sub-populations could not only produce more types of waveforms, but also the epileptic waveforms are included in them. Fig. 8 (b) illustrates the parameter distribution of (B , G) corresponding to four types of EEGs.

B2) performance verification of the model training method MTM-F-GA—In this part, we focus on verifying the feasibility and efficiency of MTM-F-GA on artificial EEG data. Here, the time delay τ is taken as an example to show the results. A sequence of τ is firstly generated based on uniform distribution, which is shown as the red line in Fig. 9. Given the generated sequence of τ and other parameters with nominal values, we can then calculate a sequence of outputs of TD-W-SP model by solving Eqs. (12). Each output is regarded as an artificial EEG here. Next, we apply the method MTM-F-GA into the artificial EEGs, the optimal values of τ can be obtained, which are shown as the blue dot line in Fig. 9. Obviously, there only exist tiny differences between the real values and optimized values of τ , which shows the good performance of the method MTM-F-GA. Note that similar results can be obtained for other parameters.

B3) performance verification of the model-driven seizure tracking method using epileptic EEGs—In this part, we will verify (1) why it is reasonable to consider parameters A , B , τ , and (2) how parameters A , B , τ work, in the aspect of exploring the evolution of “Preictal-ictal-Postictal” in epileptic EEGs.

We first validate the capability of proposed model-driven approach to recover and track parameters of interest (A , B , τ_A , τ_B) using the simulated data. Firstly, a 30s-long simulated EEG segment is generated by the proposed model TD-W-SP (see Fig. 10 (a)), where the normal-like EEG (first 10s), slow rhythmic activity (middle 10s) as well as seizure-like EEG (last 10s) are obtained respectively with different parameter settings. Note that the parameter values for each case are known a priori and served as a ground truth, which are illustrated as the black solid lines in Fig. 10 (b) – (e). Furthermore, the proposed model is trained by the simulated EEG to obtain the estimated parameter values, whose results are illustrated as the blue dotted line in Fig. 10 (b) – (e). We can observe from Fig. 10 that the proposed model-driven approach could better recover and track the parameters on simulated data.

Next, we verify the parameters A , B , τ are helpful in exploring the evolution of epileptic seizures. Given an EEG signal including three stages of a seizure (30s preictal, 20s ictal and 30s post-ictal) which are labeled by experts (see Fig. 11 (2a)), we segment it into a number of EEG segments by 2s sliding windows with 1s overlap. Then for each EEG segment, we can obtain the optimal values of parameters A , B , τ , a by Eqs. (13)–(14) respectively. The variation trend of all parameters are illustrated in Fig. 11 (2b)–(2e). Seen from Fig. 11 (2b), we can observe that there happens a rapid increase of A around 15s, and 25s later, the values of A tend to be parallel after a rapid decrease. Similar results can be obtained in the cases of B and τ if we change the increase and decrease mutually (see Fig. 11 (2c)–(2d)). However, such apparent trend has not been consistently observed in the case of a shown as in Fig. 11

(2e). These results verify that the variation trends of A , B , τ are very helpful in guiding us to explore the evolution of “Preictal-ictal-Postictal” in epileptic EEGs.

Finally, we verify the effectiveness of proposed I , TP-PI and TP-IP in the field of tracking different periods of a seizure. In order to calculate the threshold, we first select one EEG file without any seizure for each patient, and then artificially choose 200s-long continuous EEG segment without single spike or other epileptiform waves. Such obtained 200s-long EEG segment are then defined as the “normal EEG signal” for each patient. Then 100 normal (i.e. $K_{nor} = 100$) EEG segments are obtained by 2s sliding window without any overlap. In our simulation, $k_1 = 2$. Fig. 12 (a) illustrates a 80s-long EEG segment including 30s pre-ictal, 20s ictal and 30s post-ictal EEGs from “patient 1” and the sequence of its indexes. The two thresholds are 0.4 and 0.79 respectively. Then the two turning points are 2982s and 3020s, which are 14s earlier than the labeled onset time (2996s) and 4s later than the labeled off set time (3016s). Fig. 12 (b) shows a 112s-long EEG segment (30s pre-ictal, 52s ictal and 30s post-ictal EEGs) from “patient 3” and corresponding sequence of indexes. The TP-PI and TP-IP are 352s and 415s, which are 10s earlier than the labeled onset time (362s) and 1s later than the labeled off set time (414s). Also, we can observe from Fig. 12, the trend of indexes clearly reflect the cycle of seizures. On the other hand, we can regard the estimated TP-PI as an alarming time for early seizure detection. It is known that the more earlier the predicted onset time, the more timely the pre-control could be carried out. However, the more earlier the predicted off set time the more difficult the information of seizures could be captured. For each of seizure, we apply the pre-estimated duration (PRD) and the post-estimated duration (POD) to evaluate the performance of proposed method. Due to the limited space, we only list the results of one seizure for each patient (see Table 3). Table 3 shows the ictal duration whose left end is the onset time labeled by experts (LON) and right end is the off set time labeled by experts (LOF), the TP_{PI} and TP_{IP} estimated by Eqs. (18)–(19), the PRD and the POD respectively. We can observe from Table 3 that the estimated TP_{PI} generally present around 10s earlier than the labeled onset times, and the estimated TP_{IP} are 1s-4s later than the labeled off set times. For each patient, we define the “tracking accuracy (TA)” to evaluate the performance of proposed method, denoted by

$$TA = \frac{\# \{ \text{seizures satisfying } PRD > 0 \& POD > 0 \}}{\# \{ \text{all seizures of each patient} \}},$$

$$PRD = LON - TP_{PI},$$

$$POD = TP_{IP} - LOF.$$

Here, $\# \{ \text{seizures satisfying } PRD > 0 \& POD > 0 \}$ is the number of seizures satisfying $PRD > 0$ and $POD > 0$, which means TP-PI is earlier than LON and TP-IP is later than LOF (that is, the estimated ictal duration totally cover the labeled ictal duration). The corresponding results for each patient are listed in Table 3.

4. Discussion

In this work, we have presented a model-driven seizure tracking approach, where the novel proposed TD-W-SP model is trained according to two features extracted from epileptic EEGs, as well as the model parameter variation trend is characterized to explore the evolution of three stages during a period of epileptic seizure. With the understanding of the physiological interpretation for each model parameter, the obtained parameter tracking results may be helpful for researchers to explore new hypotheses of mechanisms underlying epilepsy, especially in tracking the evolution of three stages (that is, from pre-ictal to ictal and from ictal to post-ictal). Moreover, such results are also helpful for physiologists to timely capture the tiny but subtle changes in the underlying physiological processes, which may be useful in designing the treatment strategies in clinics. For example, it is possible to give a guide in determining whether or when the GABAergic (glutamatergic) drugs are required for patients, as well as in designing the electrical stimulation therapy for an epilepsy patient if needed.

There have been proposed various neural computational models to elucidate the generation of physio-pathological activities, however, they often neglect the information contained in clinic data so that there exists a big gap between the model and its applications in clinics. In recent years, there has been an increasing interest in the study of combining neural computational models with data analysis. It is worth mentioning here the work in [36], which is the latest research finding on this point. Yochum et al. proposed a model-based reverse engineering approach to reconstruct the post-synaptic potentials (PSPs) by reverse modeling of local field potential (LFP). Specifically, the LFPs were recorded with extracellular electrodes implanted in brain tissue, and fed into a neural mass model to estimate the model parameters. Then the estimated parameters were applied to reconstruct the post-synaptic potentials. It should be noted that the basic idea of reverse engineering approach in Yochum's work is similar as that in our work, that is, both of them were designed on the basis of combining the neural mass model with the real data. However, the problems to be solved in two works are quite different. Yochum's work aims to reconstruct PSPs, while our work focuses on tracking the evolution of epilepsy. Besides, the real data applied in two works are totally different. Yochum's work applied the LFPs collected from neuron assemblies directly, which could better match the model output. But the EEGs applied in our work are recorded with the noninvasive electrodes placed along the scalp, where discharges of neuron assemblies are attenuated due to the existence of soft tissue and skull, as well as contaminated due to a significant presence of environmental noise and artifacts. Under such situation, there must exist a big gap between the real EEG data and the model output so that it is difficult to apply the voltage difference between them to estimate the model parameter directly. Alternatively, an error function with respect to the extracted features from them were defined to train the model in our work.

It is necessary to clarify that in this work, we only focused on one of possible mechanisms in epilepsy, which was revealed in [33]. Indeed, there are recent evidences that different physiological interpretations are linked to occurrence of epileptic seizures [37]. Therefore, in the future study, we will follow with interesting in incorporating these latest findings into the neural computational modeling. Additionally, the on-line tracking is of great significance in

realizing the applications in clinics, where an efficient optimization algorithm in estimating the model parameters is the first step. We have started to focus on this work. Hope we can obtain the satisfactory results in the near future. Moreover, the network-level neural computational modeling is another research frontier we are going to follow, where the interaction of multiple neural populations located in different cortical areas can be represented. It will not only be helpful to simulate EEGs more similar to the real EEGs, but also helpful to understand the network-level phenomenology in epilepsy, such as the synchronization between multiple channels, spreading of epileptiform waves, anterior-posterior lag or gradient. Network-level models may provide novel insight for understanding epilepsy and realizing seizure tracking more accurately.

5. Conclusion

In this paper, we have first proposed a new time-delay Wendling model with sub-populations (TD-W-SP) according to three aspects of improvements: (1) a new response function is formulated in pyramidal population PY; (2) two time delays are added in excitatory interneuron population E and slow inhibitory interneuron population I1; and (3) each population are divided into a number of sub-populations. The proposed model TD-W-SP not only concerns the response alteration of populations PY, E, I1 which are influenced by the entry of $GABA_{A,fast}$ but also appears more effective in capturing the diversity of neuronal networks. Furthermore, we have introduced a model-driven seizure tracking approach using epileptic EEGs. In this approach, the TD-W-SP model is first trained in light of the power spectral and fractal dimension, which are extracted from epileptic EEGs in frequency domain and time domain respectively. Then an index is defined as a function of the trained model parameters and applied to characterize the trend of parameter variation. The performances of proposed methods have been verified on an EEG datasets which is built from 8 patients in CHB-MIT database. Simulation results show that the proposed model TD-W-SP performs well in simulating epileptic-like EEGs. Meanwhile, it has been verified that the index trend keep consistent with the evolution of three stages during a period of epileptic seizure, that is, from pre-ictal to ictal and from ictal to post-ictal. Moreover, the estimated TP-PI and TP-IP could be suggested to be an alarming time to carry out the pre-control timely and an indicated time to weaken the control for doctors.

Acknowledgement

This work was supported by the National Natural Science Foundation of China under Grant 61473223, the Innovative Talents Promotion Plan of Shaanxi Province under Grant 2018TD-016, and the Foundation for the National Institutes of Health of United States under Grants 1K23NS090900, 1R01NS102190, 1R01NS102574, 1R01NS107291.

References

- [1]. Birjandtalab J, Pouyan MB, Cogan D, Nourani M and Harvey J 2017 Computers in biology and medicine 82 49–58 [PubMed: 28161592]
- [2]. Song JL, Hu W and Zhang R 2016 Neurocomputing 175 383–391
- [3]. Altunay S, Telatar Z and Eroglu O 2010 Expert Systems with Applications 37 5661–5665
- [4]. Subasi A, Ercebebi E, Alkan A and Koklukaya E 2006 Computers in Biology and Medicine 36 195–208 [PubMed: 16389078]

- [5]. Guo L, Rivero D, Dorado J, Rabunal JR and Pazos A 2010 *Journal of neuroscience methods* 191 101–109 [PubMed: 20595035]
- [6]. Kumar Y, Dewal M and Anand R 2014 *Neurocomputing* 133 271–279
- [7]. Fu K, Qu J, Chai Y and Dong Y 2014 *Biomedical Signal Processing and Control* 13 15–22
- [8]. Song JL and Zhang R 2017 *Multidimensional Systems and Signal Processing* 28 945–959
- [9]. Zhang SL, Zhang B, Su YL and Song JL 2019 *International Journal of Machine Learning and Cybernetics* 1–10
- [10]. Jouny CC, Franaszczuk PJ and Bergey GK 2005 *Clinical neurophysiology* 116 552–558 [PubMed: 15721069]
- [11]. Beurle RL 1956 *Trans. Roy. Soc. (Lond) B* 240 55–94
- [12]. Lopes da Silva F, Hoeks A, Smits H and Zetterberg L 1974 *Biological Cybernetics* 15 27–37
- [13]. Wilson HR and Cowan JD 1972 *Biophysical journal* 12 1–24 [PubMed: 4332108]
- [14]. Wendling F, Bartolomei F and Chauvel P 2000 *Biol. Cybern* 83 367–378 [PubMed: 11039701]
- [15]. Zavaglia M, Astolfi L, Babiloni F and Ursino M 2006 *Journal of neuroscience methods* 157 317–329 [PubMed: 16757033]
- [16]. David O, Harrison L and Friston KJ 2005 *NeuroImage* 25 756770
- [17]. RJ M, SJ K, KE S, RB R, J D and KJ F 2007 *Neuroimage* 37 706–720 [PubMed: 17632015]
- [18]. Wang P and Knosche TR 2013 *Plos One* 8 117
- [19]. David O and Friston KJ 2003 *NeuroImage* 20 17431755
- [20]. Wendling F, Bartolomei F, Bellanger JJ and Chauvel P 2002 *European Journal of Neuroscience* 15 1499–1508 [PubMed: 12028360]
- [21]. Whittington MA, Traub R, Kopell N, Ermentrout B and Buhl E 2000 *International journal of psychophysiology* 38 315–336 [PubMed: 11102670]
- [22]. Jansen BH and Rit VG 1995 *Biological cybernetics* 73 357–366 [PubMed: 7578475]
- [23]. Geng S, Zhou W, Zhao X, Yuan Q, Ma Z and Wang J 2014 *Biological cybernetics* 108 747–756 [PubMed: 25048203]
- [24]. David O and Friston KJ 2003 *NeuroImage* 20 1743–1755 [PubMed: 14642484]
- [25]. Hocepiéd G, Legros B, Van Bogaert P, Grenez F and Nonclercq A 2013 *Computers in biology and medicine* 43 1773–1782 [PubMed: 24209923]
- [26]. Youssofzadeh V, Prasad G and KongFatt Wong-Lin 2015 *NeuroImage* 108 364–376 [PubMed: 25562823]
- [27]. Kuhlmann L, Freestone DR, Manton JH, Heyse B, Vereecke HE, Lipping T, Struys MM and Liley DT 2016 *NeuroImage* 133 438456
- [28]. Roessgen M, Zoubir BAM and Boashash B 1998 *IEEE TRANSACTIONS ON BIOMEDICAL ENGINEERING* 45 673–685 [PubMed: 9609933]
- [29]. Pérez-Gussinyé M, Swain C, Kirby J and Lowry A 2009 *Geochemistry, Geophysics, Geosystems* 10
- [30]. Esteller R, Vachtsevanos G, Echaz J, Henry T, Pennell P, Epstein C, Bakay R, Bowen C and Litt B 1999 *Fractal dimension characterizes seizure onset in epileptic patients icassp (IEEE) pp* 2343–2346
- [31]. Whitley D 1994 *Statistics and computing* 4 65–85
- [32]. Hocepiéd G, Legros B, Bogaert PV, Grenez F and Nonclercq A 2013 *Computers in Biology and Medicine* 43 1773–1782 [PubMed: 24209923]
- [33]. Karoly PJ, Kuhlmann L, Soudry D, Grayden DB and Freestone DR 2018 *PLoS Computational Biology* 14
- [34]. Shoeb, AH, Application of machine learning to epileptic seizure onset detection and treatment. Massachusetts Institute of Technology; 2009. Ph.D. thesis
- [35]. Chen LL, Zhang J, Zou JZ, Zhao CJ and Wang GS 2014 *Biomedical Signal Processing and Control* 10 1–10
- [36]. Yochum M, Modolo J, Mogul D, Benquet P and Wendling F 2019 *Journal of neural engineering*
- [37]. Elahian B, Lado NE, Mankin E, Vangala S, Misra A, Moxon K, Fried I, Sharan A, Yeasin M, Staba R et al. 2018 *Annals of neurology* 84 588–600 [PubMed: 30179277]

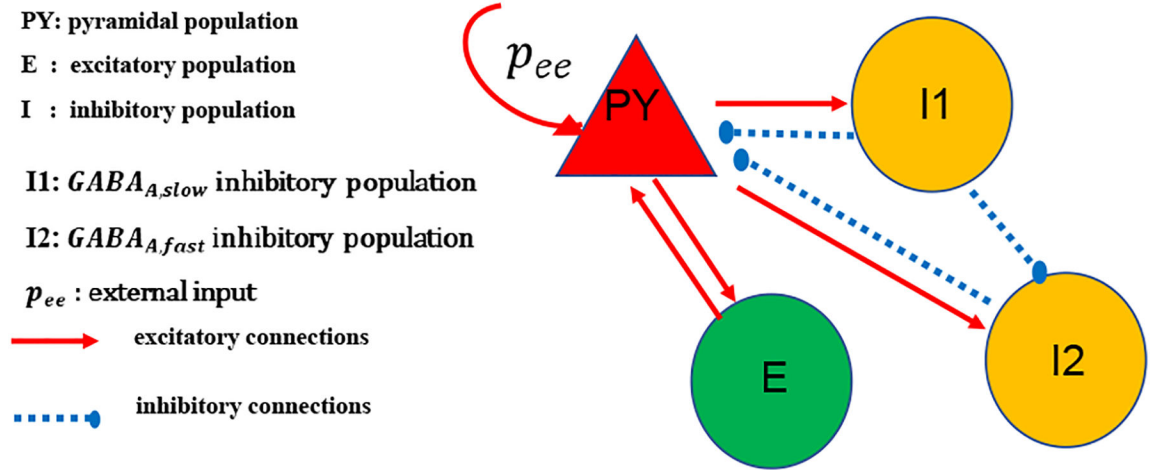


Figure 1.
The topological structure of Wendling model

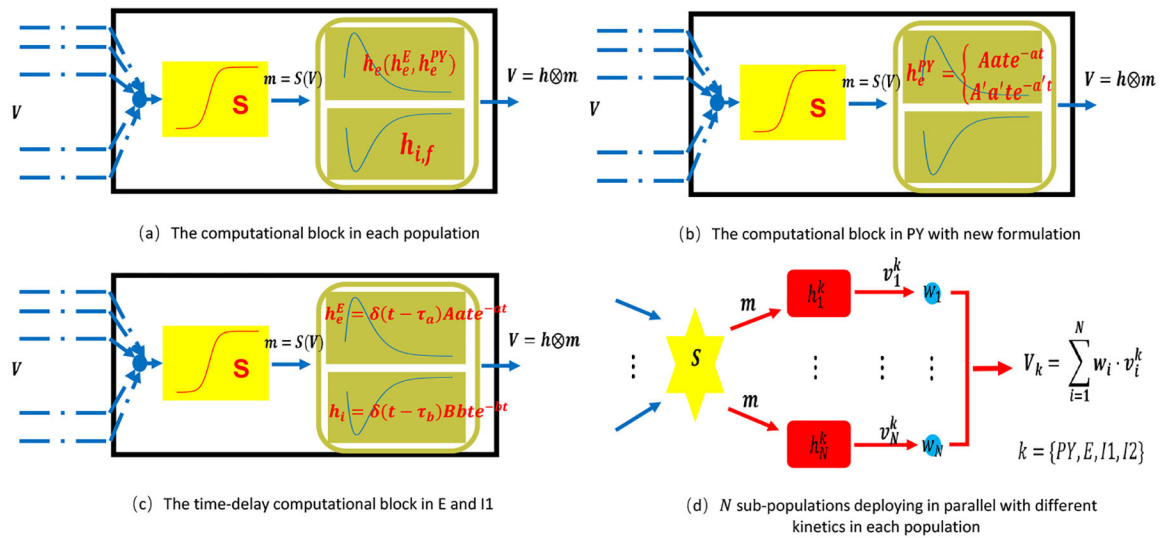


Figure 2.

(a) The computational block in each population; (b) The computational block in PY with new formulation; (c) The time-delay computational block in E and I1; (d) N sub-populations deploying in parallel with different kinetics in each population.

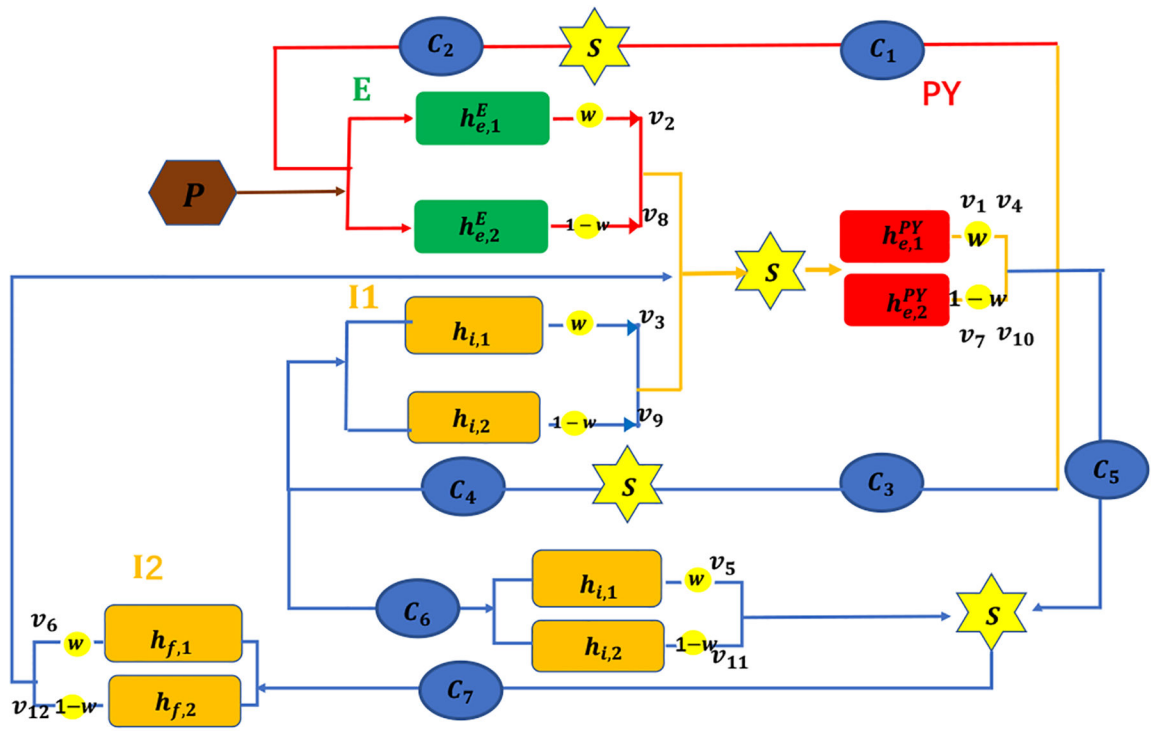


Figure 3.
The neuronal population organization of TD-W-SP model

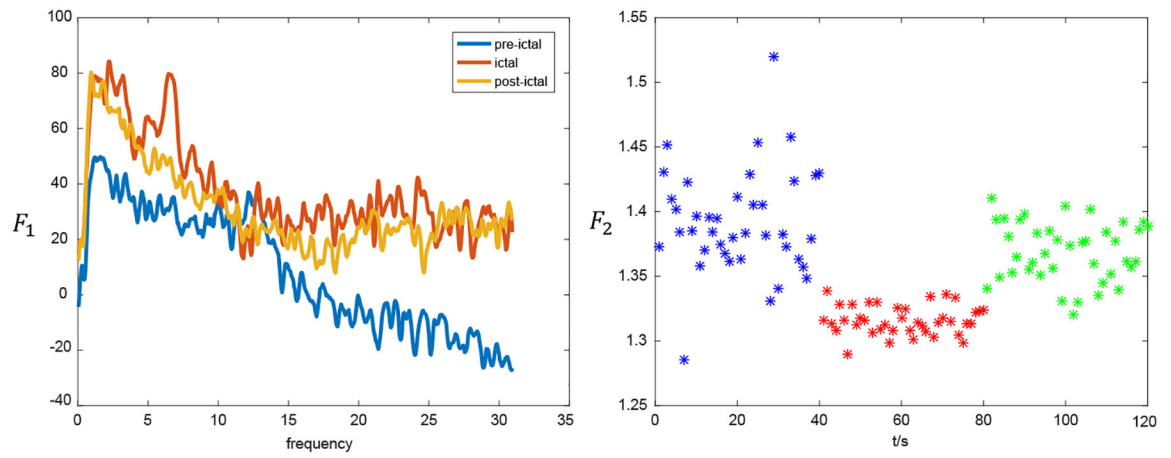


Figure 4.
(a) The power spectral of pre-ictal, ictal and post-ictal EEGs; (b) The fractal dimension on pre-ictal, ictal and post-ictal EEGs

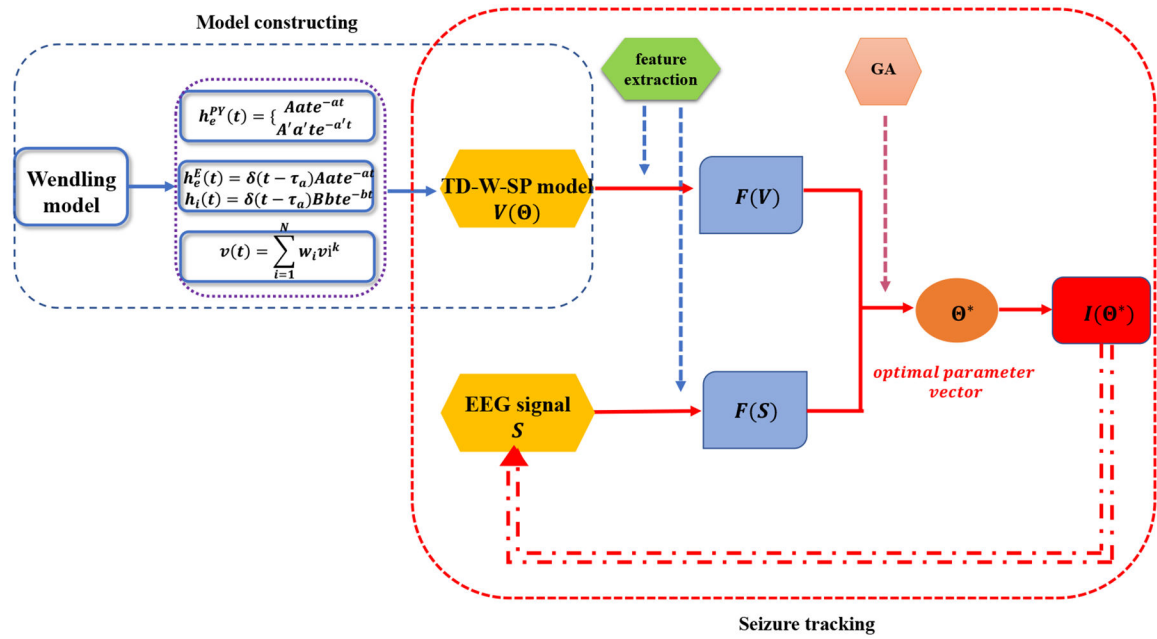


Figure 5. The procedure of TD-W-SP model and model-driven seizure tracking approach using epileptic EEGs.

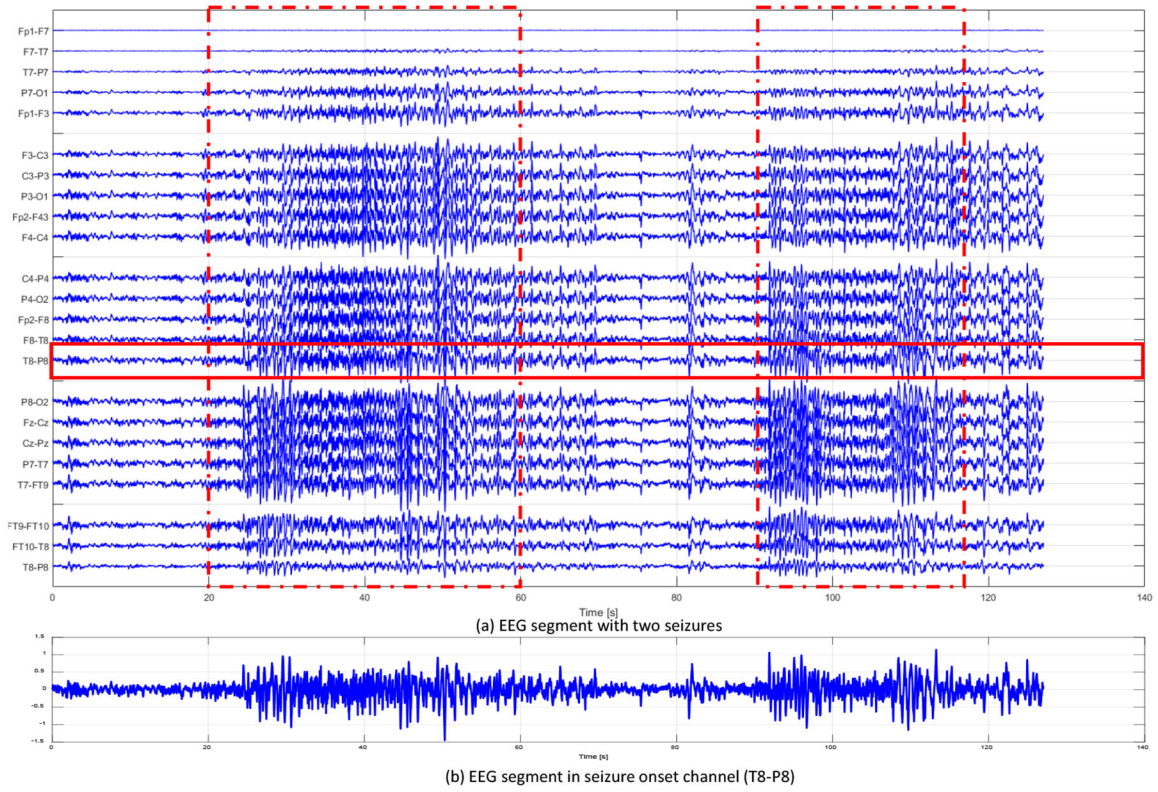


Figure 6. (a)An EEG segment with two seizures for “patient 1”; (b) Corresponding signals in seizure onset channel (T8-P8).

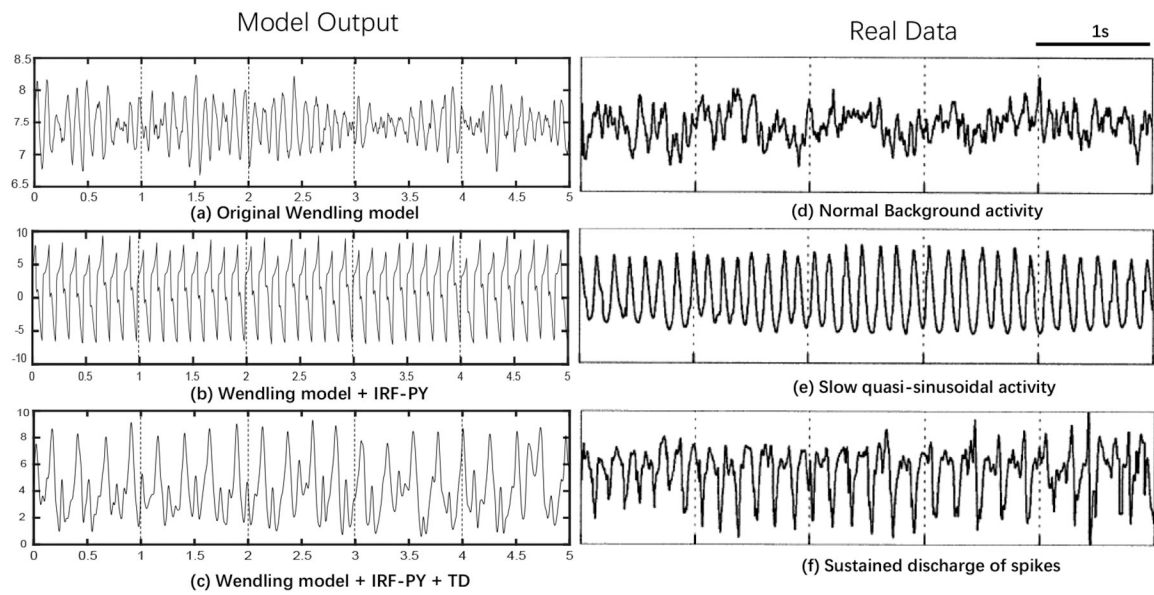


Figure 7.

(a)-(c) The outputs of original Wendling model, “Wendling + IRF-PY” and “Wendling + IRF-PY + TD”;(d)-(f) Real depth-EEG signals recorded in human hippocampus (during SEEG exploration and using intracerebral multiple lead depth-electrodes) in [20].

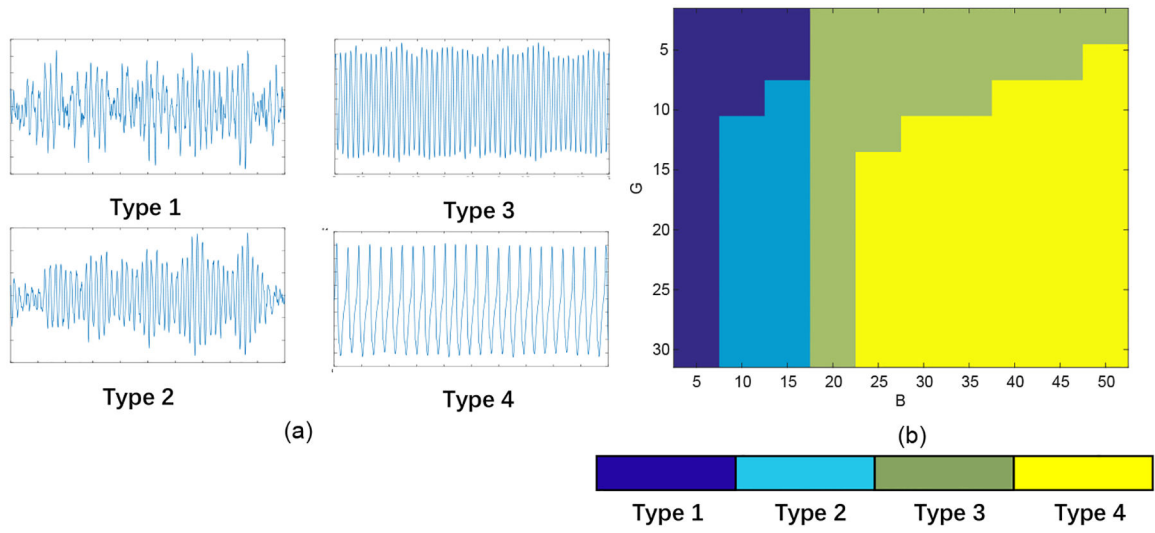


Figure 8.
The outputs of “Wendling + SP” and the corresponding parameter distribution

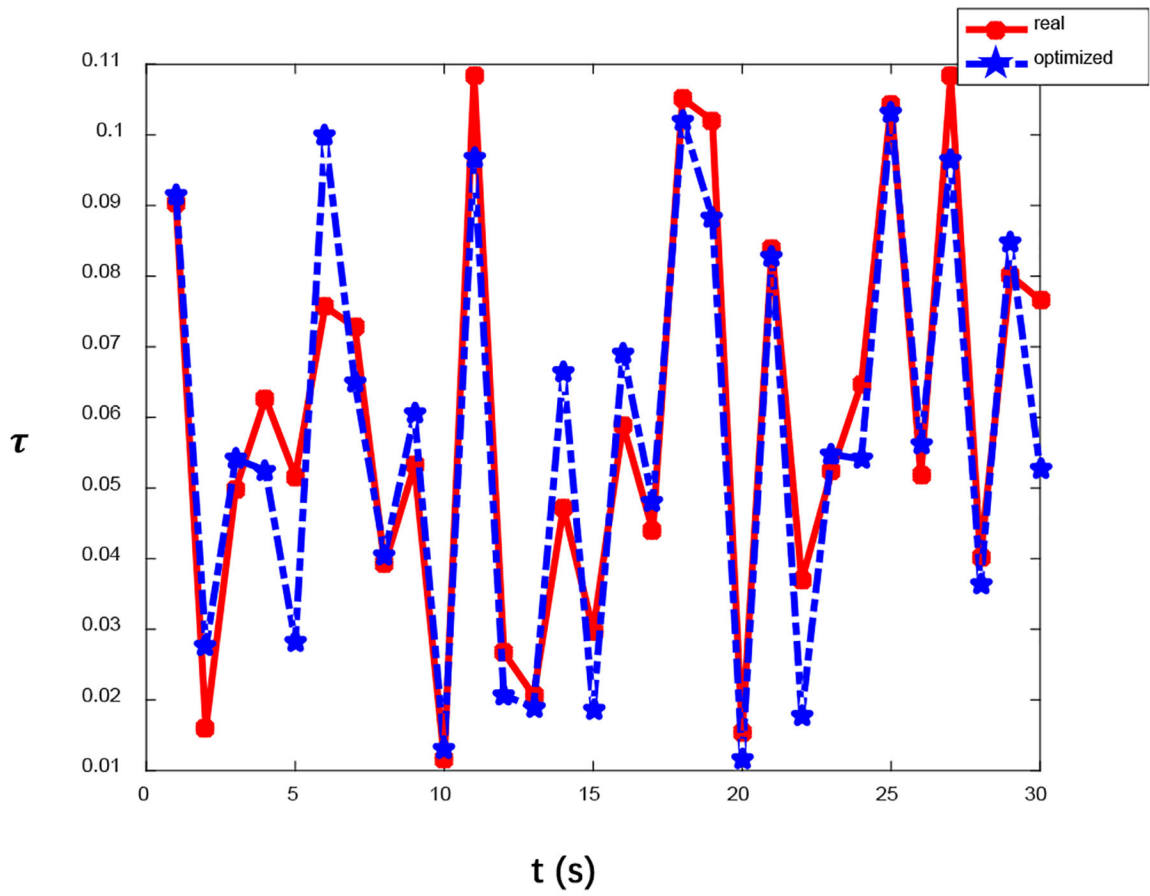


Figure 9.
Comparison between the real values and the optimized values of τ by MTM-F-GA

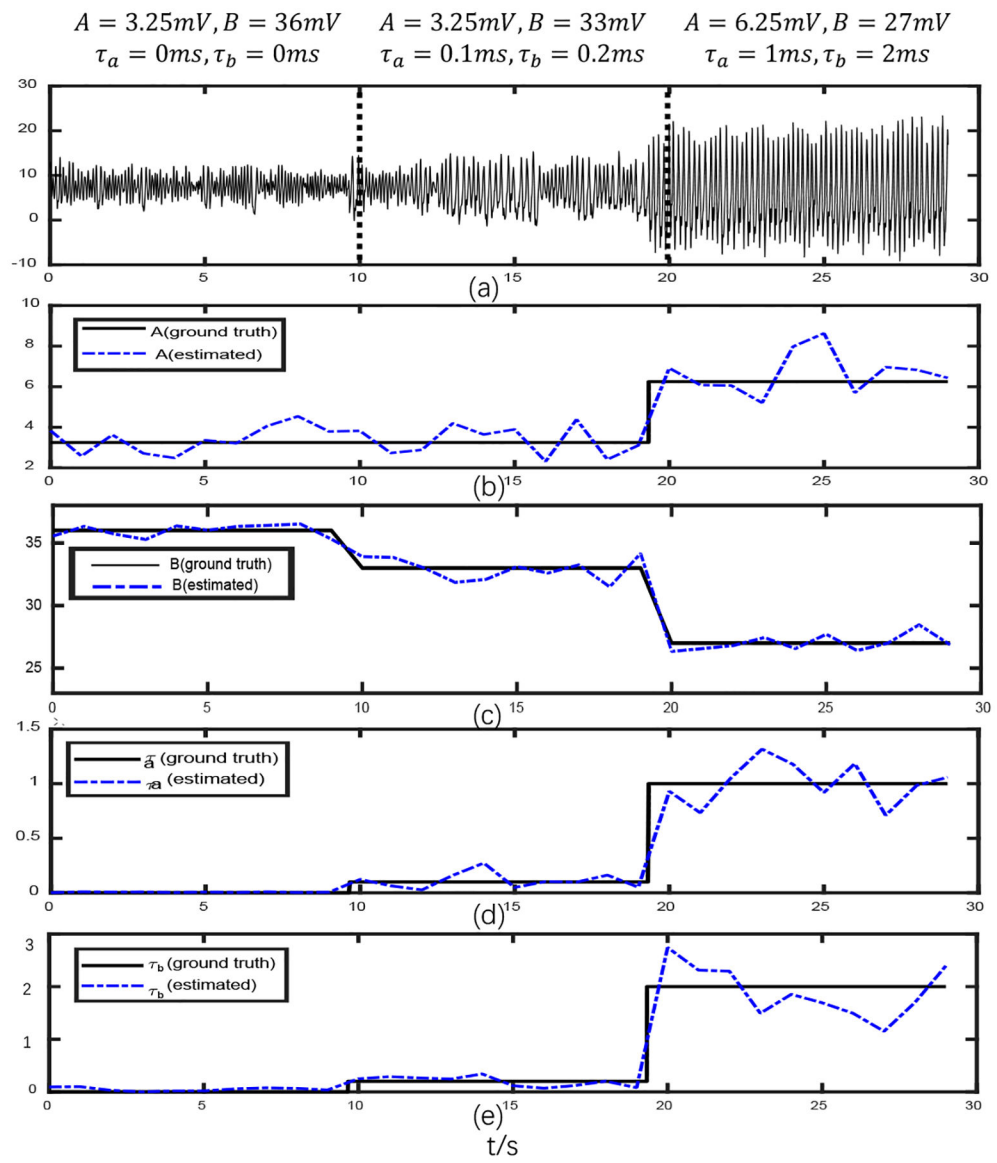


Figure 10. The 30s simulated EEG segment and the corresponding values for parameters A, B, a, τ_b (ground truth and estimated values).

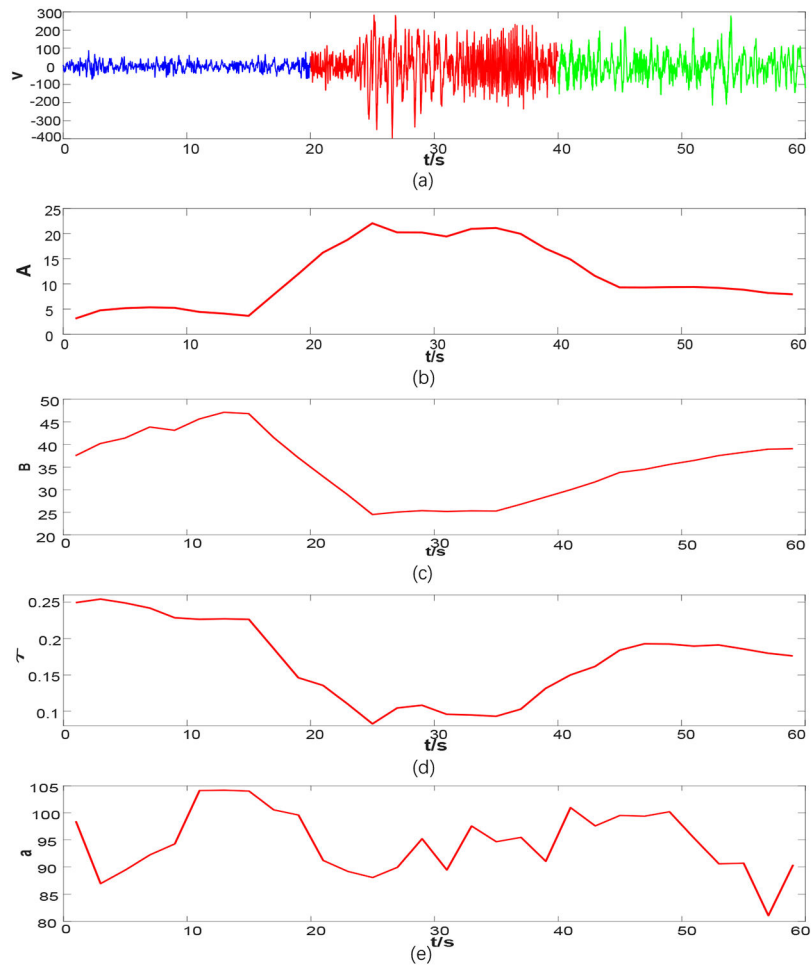


Figure 11.
An EEG segment and the variation trends of A , B , τ , a

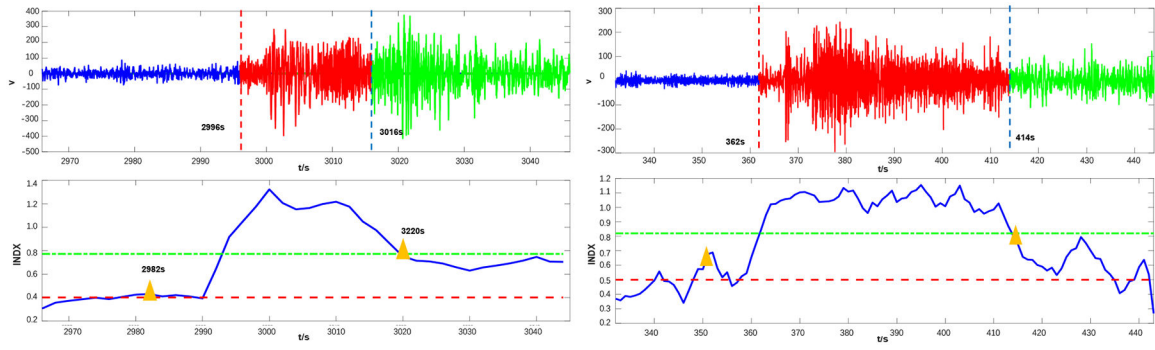


Figure 12.
 (a) A 80s-long EEG segment from “patient 1” and the sequence of its indexes; (b) A 112s-long EEG segment from “patient 3” and the sequence of its indexes.

Table 1.

Detail information of EEG dataset in our simulations

Patient	Basic information			EEG dataset		
	Age(years)	Duration(hr)	No. of channels	the selected channel	No. of seizures	total duration(s)
1	11	44	23	T8-P8	7	442
2	11	34	23	T8-P8	3	172
3	14	38	23	T7-P7	7	402
4	22	42	24	T7-P7	4	378
5	7	39	23	F7-T7	5	558
6	3.5	20	23	T7-P7	5	919
7	10	19	24	F7-T7	4	276
8	3	25	23	T7-P7	7	447

Author Manuscript

Author Manuscript

Author Manuscript

Author Manuscript

Table 2.

The nominal value of parameters in TD-W-SP model

Parameter	Nominal value	Unit
A, A'	3.25	mv
B	22	mv
G	10	mv
a, a'	100	s^{-1}
b	50	s^{-1}
g	500	s^{-1}
C	135	/
v_0	6	mv
e_0	2.5	s^{-1}
v_0	0.56	mv^{-1}

Author Manuscript

Author Manuscript

Author Manuscript

Author Manuscript

Table 3.

Performances of the model-driven seizure tracking method

Patient	labeled ictal duration (s)	TP_{PI} (s)	TP_{IP} (s)	PRD (s)	POD (s)	TA
1	(2996, 3016)	2982	3020	14	4	0.86
2	(3369, 3378)	3367	3381	3	3	1
3	(362, 414)	352	415	10	1	0.71
4	(7804, 7853)	7796	7857	8	4	1
5	(1086, 1196)	1077	1198	11	2	0.8
6	(2670, 2841)	2657	2842	13	1	1
7	(12231, 12295)	12228	12298	10	3	0.75
8	(6313, 6348)	6304	6349	9	1	0.86

Author Manuscript

Author Manuscript

Author Manuscript

Author Manuscript